Zeitschrift für Kristallographie, Bd. 129, S. 65–83 (1969)

The crystal structure of orthoenstatite

By NOBUO MORIMOTO and KICHIRO KOTO

Institute of Scientific and Industrial Research
Osaka University, Suita, Osaka, Japan

(Received February 22, 1968)

Auszug

Die Kristallstruktur eines Enstatits (Orthoenstatits) aus dem Meteoriten von Bishopville wurde aus 680 *hkl*-Interferenzen mittels der Ausgleichsmethode verfeinert. Die Gitterkonstanten sind $a = 18{,}210$, $b = 8{,}812$ und $c = 5{,}178$ Å; Raumgruppe ist *Pbca*.

Die Struktur des Enstatits wird mit der des Klinoenstatits verglichen; die geometrischen Beziehungen zwischen beiden Modifikationen werden untersucht. Die rhombische Elementarzelle des Enstatits erwies sich als aufgebaut aus zwei monoklinen Zellen des Klinoenstatits, die durch eine *b*-Gleitspiegelungsebene parallel (100) verzwillingt sind. Die Enstatit-Struktur wurde auch mit den Strukturen von Hypersthen und Orthoferrosilit verglichen. Es zeigte sich, daß mit wachsendem Eisengehalt die Abstände Metall–Sauerstoff in den Oktaedern um die Metallatome zunehmen. Die Abstände können daher zur Ermittlung des Verhältnisses Mg:Fe dienen. Überraschend ist die Abnahme der Si–O-Abstände in den Tetraedern um Si mit zunehmendem Gehalt von Fe in den Mg-Lagen.

Abstract

The crystal structure of a natural orthorhombic enstatite (orthoenstatite) from the Bishopville meteorite, has been refined by the least-squares method using 680 three-dimensional reflections. The space group and the cell dimensions of this orthoenstatite are *Pbca* and $a = 18.210$, $b = 8.812$ and $c = 5.178$ Å.

The crystal structure of orthoenstatite is compared with that of clinoenstatite and the geometric relationship between the two polymorphs is described. The orthoenstatite structure is shown to be an exact twin of clinoenstatite on a unit-cell scale. The orthorhombic cell is composed of two monoclinic cells of clinoenstatite joined on (100) through a *b*-glide plane.

The orthoenstatite structure is also compared with the structures of hypersthene and orthoferrosilite. The corresponding interatomic distances show the following characteristics. With increasing Fe replacement of Mg the interatomic distances M–O in the metal octahedra increase. The mean interatomic distances, M–O, of the octahedra can thus be used to determine the Mg:Fe

ratio in the octahedral sites. More surprisingly, an increase of Fe in Mg positions is accompanied by a decrease of the mean Si—O distances in the silicate tetrahedra.

Introduction

The phase relations of $MgSiO_3$ have been extensively studied because of their important implications in petrology (BOYD and SCHAIRER, 1964; SCLAR *et al.*, 1964). However, many questions on it remain unanswered. The precise determinations and the comparison of the crystal structures of two polymorphs of $MgSiO_3$, i.e., orthoenstatite and clinoenstatite, should help us to understand the crystal chemistry of pyroxenes in general.

The crystal structure of an orthorhombic pyroxene was first determined by WARREN and MODELL (1930), who studied hypersthene of composition $En_{70}Fs_{30}$. They found that hypersthene contains the typical SiO_3 chains similar to those of diopside (WARREN and BRAGG, 1928), and that the main structural difference between hypersthene and diopside is the stacking of the SiO_3 chains parallel to (100). Thus the orthorhombic unit cell could be considered as composed of two monoclinic cells joined on the (100) through a *b*-glide plane. The structure of a nearly pure orthoenstatite was shown by BYSTRÖM (1943) to be similar to that of hypersthene.

ITO (1935, 1950) studied the structure of bronzite with a composition of $En_{84}Fs_{16}$ using the hypothesis that orthorhombic pyroxenes must be a cell twin of monoclinic pyroxene, that is, the orthorhombic unit cell must be composed of two monoclinic unit cells twinned by a *b*-glide plane parallel to (100). At that time, however, knowledge of the structure of the monoclinic pyroxenes was not very detailed and the only known structure of the monoclinic pyroxenes was that of diopside. The comparison of the structure of bronzite determined by two-dimensional data and that of diopside showed that only in approximation could orthopyroxenes be regarded as twinned diopside.

However, results obtained by ITO on the structure of bronzite showed the possible existence of clinopyroxenes with a space group different from that of diopside. It was later discovered that clinopyroxenes, which have polymorphic relationships with orthorhombic pyroxenes, belong to space group $P2_1/c$ rather than $C2/c$, the space group of diopside (MORIMOTO, 1956; BOWN and GAY, 1957). MORIMOTO, APPLEMAN and EVANS (1960) determined the crystal structures of clinoenstatite and pigeonite and found that there were two crystallographically different SiO_3 chains in the structure of clinoenstatite,

as in that of orthoenstatite. These results indicated the possibility that the orthopyroxenes might be more correctly related in structure to twinned clinoenstatite and pigeonite. Though BROWN *et al.* (1961) discussed the structural relationship of the three polymorphs of $MgSiO_3$, the refinement of the structures of the $MgSiO_3$ polymorphs has been left for later work. LINDEMANN (1961) published the atomic coordinates for orthoenstatite based on two-dimensional intensity data.

The present study was initiated to refine the crystal structure of orthoenstatite in order to elucidate the following problems:

1. The extent to which the structure of orthoenstatite could be regarded as that of clinoenstatite twinned on a unit cell scale.
2. The effect of Fe atoms replacing Mg atoms in the pyroxene structure by comparing the structural relations between orthoenstatite and hypersthene.

While this work was in progress, many investigations of the crystal structures of pyroxenes have been published. GHOSE (1965) refined the structure of hypersthene with composition $En_{47}Fs_{53}$ from a metamorphic rock. His results showed almost complete ordering of Mg and Fe atoms in the structure. BURNHAM (1967) refined the structures of orthoferrosilite and clinoferrosilite and discussed their structural relationships.

Experimental

Single crystals of orthoenstatite from the Bishopville meteorite, kindly given by Dr. H. S. YODER, JR., Geophysical Laboratory, Washington, D. C., have been used for the present structure refinement. Because the structural study of clinoenstatite (MORIMOTO *et al.*, 1960) was made with a specimen obtained by heating orthoenstatite from the Bishopville meteorite at 1400°C for 24 hours, the chemical composition should be the same for the two polymorphs and a comparison of their structures is possible. The chemical composition of this orthoenstatite is reported to be $MgSiO_3$ with 0.1 to 1.0 percent each of Al, Ca and Fe as well as 0.01 to 0.1 percent each of Cr, Mn, Na and Ti (SWANSON *et al.*, 1956).

The cell dimensions were determined using the powder method with quartz and silicon as internal standards. The wavelength of Cu$K\alpha$ was taken equal to 1.5418 Å. The values obtained are: $a = 18.210 \pm 0.010$, $b = 8.812 \pm 0.005$ and $c = 5.178 \pm 0.004$ Å. They are in agreement with the results obtained by POLLACK and

RUBLE (1964) and STEPHENSON *et al.* (1966) within experimental error. The space group is *Pbca*. A needle crystal, $0.24 \times 0.09 \times 0.08$ mm^3 in size, was used for collecting the intensity data with Cu$K\alpha$ radiation. Three-dimensional data for 917 crystallographically independent reflections were collected using Weissenberg photographs taken around the *b* and *c* axes. The relative intensities were measured visually by means of the multiple-film technique and corrected for the polarization and Lorentz factors. No absorption correction was made. Reflections from different layers were correlated first by Weissenberg photographs taken around different axes and later by the computer program ORFLS (BUSING, MARTIN and LEVY, 1962).

Structure refinement

Of the 917 non-equivalent reflections measured, 237 had intensities less than background and were not used during the procedures of refinement. Structure refinement was started with the two-dimensional difference-Fourier method using 109 *hk*0 reflections. The *x* and *y* parameters obtained were found to be very similar to those given by LINDEMANN (1961). These *x* and *y* parameters were, therefore, used as the starting values, together with the *z* parameters obtained by LINDEMANN, for the least-squares refinement.

The refinement was carried out on the IBM 7090 computer using the full-matrix least-squares program, ORFLS. The scattering curves for Si, Mg and O were taken from the International tables for x-ray crystallography (1962, 258—260). Isotropic temperature factors

Table 1. *Atomic coordinates and isotropic temperature factors*
The standard deviations given between parentheses are expressed in units of the last digit stated

	x/a	*y/b*	*z/c*	*B*
M(1)	0.3760 (2)	0.6544 (4)	0.8663 (8)	0.69 (7)
M(2)	0.3769 (2)	0.4854 (4)	0.3609 (8)	0.77 (7)
Si(A)	0.2716 (2)	0.3411 (4)	0.0494 (6)	0.56 (6)
Si(B)	0.4740 (2)	0.3373 (4)	0.7988 (6)	0.64 (6)
O(1A)	0.1832 (4)	0.3386 (10)	0.0349 (16)	0.69 (13)
O(2A)	0.3118 (5)	0.5022 (10)	0.0430 (17)	0.97 (14)
O(3A)	0.3036 (5)	0.2252 (10)	−0.1698 (19)	1.14 (15)
O(1B)	0.5628 (4)	0.3382 (9)	0.8009 (16)	0.67 (13)
O(2B)	0.4337 (4)	0.4841 (9)	0.6880 (17)	0.71 (13)
O(3B)	0.4470 (4)	0.1961 (9)	0.6004 (17)	0.97 (15)

Table 2. *Observed and calculated structure factors*

h	k	l	F_o	F_c	h	k	l	F_o	F_c	h	k	l	F_o	F_c	h	k	l	F_o	F_c
4	0	0	6.4	7.2	10	1	1	5.8	- 6.9	3	7	1	23.3	- 23.8	11	2	2	14.0	- 9.6
6			16.6	- 18.8	11			23.3	- 24.2	4			17.5	20.9	12			14.0	- 11.7
8			54.3	- 50.8	12			17.5	19.4	5			34.9	42.3	13			28.9	- 30.8
12			148.1	-148.3	13			15.0	17.3	6			27.4	30.7	14			24.5	- 25.8
14			27.6	- 28.9	14			37.4	34.5	7			19.1	- 22.9	15			26.3	- 25.8
16			115.0	103.0	15			27.4	- 30.1	8			27.4	33.0	17			28.9	- 27.0
18			25.8	3.0	16			24.9	28.0	9			43.2	45.1	18			49.1	- 41.0
20			132.5	-120.6	19			11.6	- 13.4	10			11.6	12.8	19			36.8	28.6
22			10.1	- 6.5	21			19.1	17.7	11			21.6	- 23.6	20			14.0	10.9
2	1	0	10.1	- 11.8	22			9.1	- 7.0	12			29.1	32.9	21			15.8	- 14.3
4			8.3	9.8	1	2	1	93.9	71.5	13			9.1	14.5	1	3	2	9.6	- 7.7
6			167.4	191.6	2			131.3	-126.7	14			5.8	- 3.5	3			35.0	- 30.2
8			3.7	0.5	3			98.1	- 97.5	15			17.5	- 19.0	4			26.3	- 26.8
10			97.5	94.9	4			90.6	- 85.8	16			23.3	22.9	5			22.8	23.5
14			91.1	89.5	5			93.4	89.1	0	8	1	19.1	- 22.5	6			9.6	7.1
18			23.9	- 22.5	6			9.1	- 14.7	1			27.4	31.7	7			14.0	- 14.9
20			19.3	- 21.2	7			50.7	53.1	2			60.7	- 65.7	8			14.0	- 16.0
22			16.6	19.5	8			50.7	54.3	3			82.3	- 84.7	9			18.4	14.3
0	2	0	71.8	- 66.4	10			21.6	22.8	4			64.8	- 68.2	11			12.3	12.4
4			127.9	-126.6	11			11.6	- 16.5	5			43.2	46.3	15			7.9	8.7
6			10.1	- 12.0	12			29.1	- 33.4	6			15.0	- 15.2	17			7.9	- 6.8
8			32.2	33.7	13			33.2	36.2	7			23.3	25.9	19			6.1	- 6.7
10			19.3	17.8	14			11.6	9.0	8			56.5	71.0	0	4	2	15.8	- 16.0
12			10.1	10.1	15			24.9	28.2	9			7.5	- 9.9	1			30.7	33.6
14			8.3	11.0	16			49.0	48.5	10			7.5	11.0	2			63.9	61.4
16			54.3	52.9	17			44.9	- 37.7	12			13.3	- 16.6	3			41.2	- 44.0
18			10.1	4.2	18			33.2	37.4	13			34.9	35.8	5			12.3	- 14.6
20			8.3	- 5.9	19			7.5	10.8	15			29.1	33.6	6			39.4	39.8
22			8.3	- 10.9	20			9.1	5.4	16			19.1	26.0	7			35.0	34.7
2	3	0	36.8	- 30.5	21			34.9	- 30.5	1	9	1	29.1	- 35.8	8			12.3	- 6.5
4			27.6	28.1	22			44.9	42.7	2			30.7	- 39.7	9			14.0	- 11.3
6			38.6	- 38.5	1	3	1	129.6	-113.3	4			7.5	8.8	12			12.3	- 7.7
10			19.3	21.3	2			46.5	- 49.3	5			7.5	12.0	13			18.4	- 15.9
12			14.7	- 17.7	3			44.9	- 42.7	6			7.5	9.8	14			22.8	- 25.0
14			38.6	35.3	4			39.1	41.1	8			39.1	- 38.2	15			7.9	- 6.8
18			10.1	11.5	5			99.7	91.6	9			52.4	- 56.6	16			7.9	- 7.0
22			14.7	- 13.8	6			112.2	111.3	10			59.0	- 58.8	17			15.8	- 13.2
0	4	0	10.1	- 8.6	8			72.2	- 73.6	11			64.8	66.0	18			39.4	- 31.1
2			14.7	- 14.8	9			99.7	- 97.3	12			66.5	- 68.5	19			9.6	7.6
4			73.6	- 73.2	10			141.3	-146.7	13			17.5	- 21.4	20			9.6	7.0
6			6.4	10.2	11			178.7	162.1	0	10	1	29.1	33.4	1	5	2	8.8	- 7.9
8			58.0	- 63.5	12			131.3	-124.3	1			34.9	- 40.9	2			18.4	- 19.0
10			38.6	35.9	13			34.9	- 36.7	2			17.5	20.9	3			91.1	97.9
14			12.9	10.3	15			15.0	16.8	3			11.6	9.6	4			9.6	9.4
15			67.2	62.8	16			17.5	- 19.6	4			5.8	6.5	5			36.8	35.3
18			12.9	- 10.4	17			52.4	- 54.0	5			11.6	- 12.0	6			14.0	- 3.1
20			58.0	47.0	18			24.9	- 30.0	6			15.0	20.7	7			15.8	- 16.6
2	5	0	121.4	111.9	19			15.0	17.7	8			7.5	9.5	8			78.8	82.1
4			7.4	- 8.3	20			19.1	20.3	10			5.8	8.7	9			85.0	- 88.1
6			108.6	-108.4	21			46.5	43.2	0	0	2	23.3	- 19.0	11			55.2	54.2
8			10.1	- 12.3	22			59.0	61.6	1			17.5	18.2	12			86.7	93.0
10			71.8	- 77.8	0	4	1	13.3	- 8.7	2			153.3	-188.1	13			12.3	13.2
12			8.3	12.0	1			82.3	- 68.2	3			65.7	65.6	14			7.9	9.5
14			150.0	-152.2	2			74.8	78.0	4			22.8	20.0	15			18.4	- 18.2
16			10.1	14.1	3			24.9	30.0	5			153.3	-156.6	16			35.0	29.5
18			34.0	34.1	4			29.1	34.2	6			12.3	9.2	17			35.2	- 47.3
20			27.6	26.1	5			60.7	- 66.0	7			80.6	- 77.4	18			20.1	- 17.1
0	6	0	304.5	299.0	6			21.6	24.8	8			6.1	- 6.1	19			12.3	10.1
2			14.7	19.9	7			21.6	- 29.3	9			111.3	107.1	1	6	2	12.3	- 11.6
6			10.1	- 18.3	8			9.1	13.2	10			26.3	23.9	2			124.4	-129.8
8			38.6	36.5	9			13.3	- 13.1	11			167.3	162.3	3			76.2	77.6
10			19.3	- 23.6	10			7.5	- 8.6	12			32.4	30.4	4			14.0	14.0
12			73.6	- 72.3	13			7.5	- 10.8	15			24.5	- 24.5	5			78.8	- 71.6
14			19.3	- 21.9	14			19.1	- 19.5	17			68.3	58.9	7			45.6	- 46.0
16			41.4	43.5	16			29.1	- 35.7	18			47.3	42.1	8			15.8	- 14.6
2	7	0	16.6	15.9	17			17.5	22.3	19			9.6	2.6	9			88.5	89.8
4			41.4	44.4	18			27.4	- 30.1	20			9.6	6.8	10			28.9	28.3
6			43.2	42.7	19			21.6	- 21.3	21			22.8	- 20.2	11			80.6	82.4
8			12.0	10.3	20			23.3	- 20.5	22			95.5	83.2	12			18.4	15.7
10			73.6	76.6	21			24.9	26.4	1	1	2	6.1	4.3	15			14.0	- 13.1
12			14.7	- 18.6	1	5	1	11.6	10.0	2			12.3	- 10.6	16			12.3	8.3
14			56.1	47.4	2			38.9	- 41.1	3			20.1	- 23.2	17			30.7	26.4
16			8.3	- 11.1	3			19.1	20.9	4			36.8	30.8	18			24.5	23.5
18			8.3	11.1	4			29.1	33.8	5			80.6	- 74.6	1	7	2	7.9	- 10.2
0	8	0	21.2	20.3	5			40.7	41.8	6			22.8	- 17.8	2			12.3	- 8.3
2			21.2	- 27.7	6			17.5	18.9	7			6.1	4.9	3			15.8	- 16.6
4			47.8	- 50.1	7			33.2	- 34.6	8			76.2	- 74.4	4			18.4	- 15.4
8			12.9	11.9	8			19.1	23.4	9			45.6	44.8	7			30.7	- 34.2
10			21.2	26.4	9			15.0	- 20.0	10			9.6	10.7	8			45.6	- 47.4
12			6.4	- 12.4	10			11.6	- 12.5	11			85.0	- 78.5	11			18.4	- 18.8
16			38.6	37.7	11			7.5	- 9.4	12			121.8	-105.4	12			53.4	- 54.2
2	9	0	12.9	4.3	13			7.5	10.1	13			32.4	25.0	13			24.5	22.7
6			8.3	7.4	14			40.7	47.3	14			12.3	4.9	16			22.8	- 22.7
10			14.7	24.9	15			17.5	- 20.9	15			12.3	- 0.9	1	8	2	18.4	21.7
12			21.2	- 7.3	16			11.6	17.7	16			49.1	- 45.6	3			18.4	19.4
14			1.8	25.2	0	6	1	21.6	25.6	17			68.3	59.1	4			7.9	9.3
0	10	0	62.6	- 56.7	1			24.9	- 28.0	18			14.0	10.4	5			12.3	- 11.3
4			32.2	- 32.8	2			7.5	5.1	19			9.6	9.8	6			18.4	18.8
8			38.6	- 37.2	3			27.4	29.3	20			18.4	13.1	7			22.8	- 22.1
2	11	0	43.2	52.0	4			7.5	6.5	21			9.6	6.8	9			15.8	15.1
4			10.1	18.0	6			11.6	13.9	22			12.3	12.4	10			9.6	8.7
1	1	1	15.0	16.2	8			7.5	- 10.7	0	2	2	9.6	8.9	11			6.1	9.9
2			15.0	- 15.4	9			7.5	8.0	3			33.0	33.7	13			24.5	- 25.3
3			1.7	- 4.9	11			7.5	- 11.7	4			14.0	15.3	14			12.3	- 12.5
4			60.7	56.0	12			15.0	- 18.8	5			7.0	- 4.7	1	9	2	14.0	- 13.3
5			78.1	71.0	13			7.5	- 8.0	6			63.9	58.0	2			12.3	- 10.5
6			33.2	35.4	14			7.5	- 10.8	7			65.7	- 61.4	3			14.0	- 8.0
7			43.2	- 44.2	15			7.5	- 8.7	8			22.8	- 21.2	4			14.0	- 13.3
8			39.1	39.9	1	7	1	11.6	9.3	9			51.7	48.7	8			15.8	- 17.3
9			15.0	15.9	2			21.6	23.1	10			36.8	32.7	9			15.8	13.5

Table 2. *(Continued)*

h	k	l	F_o	F_c	h	k	l	F_o	F_c	h	k	l	F_o	F_c	h	k	l	F_o	F_c
10	9	2	12.3	12.2	15	4	3	24.0	23.5	16	0	4	62.7	- 58.2	2	7	4	12.5	- 7.0
12			14.0	- 15.2	16			8.3	5.5	18			17.9	- 16.9	3			31.3	28.5
2	10	2	45.6	44.4	18			11.6	- 10.7	1	1	4	55.5	68.8	5			17.9	18.2
3			35.0	- 35.2	19			11.6	- 13.3	2			11.6	13.0	9			23.3	21.8
6			20.1	22.9	1	5	3	19.0	17.2	3			33.1	35.5	10			18.8	20.8
7			18.4	- 21.6	2			43.0	- 42.7	5			60.9	56.6	11			41.2	- 40.8
8			9.6	- 11.7	3			56.2	- 55.1	6			37.6	- 38.6	0	8	4	13.4	- 15.8
1	1	3	5.0	8.2	4			16.5	- 13.7	7			51.0	- 48.0	3			7.2	10.3
2			33.9	- 38.4	5			10.8	- 10.6	9			25.1	22.2	4			15.2	17.0
3			49.6	- 53.4	6			28.9	- 26.7	10			65.3	65.6	5			25.1	27.2
5			16.5	- 17.1	7			13.2	- 14.0	11			51.0	- 54.7	8			23.3	- 26.3
6			43.0	- 42.0	9			24.0	22.8	13			13.4	15.8	1	1	5	15.1	12.5
7			30.6	- 30.9	10			24.0	- 22.9	14			18.8	17.4	3			17.6	16.2
9			26.5	24.2	13			8.3	- 9.8	15			37.6	- 31.6	4			14.3	13.6
10			40.5	- 38.0	14			13.2	12.2	18			21.5	19.4	5			17.6	16.5
11			9.9	- 13.0	15			33.9	29.6	0	2	4	17.9	- 17.3	6			34.4	- 37.1
13			14.9	12.5	16			8.3	9.9	1			29.5	30.0	7			16.8	18.7
14			14.9	- 13.2	17			20.7	23.3	4			15.2	17.1	8			16.8	20.4
15			16.5	21.3	18			11.6	- 15.3	5			59.1	56.3	9			13.4	12.7
17			33.9	33.5	2	6	3	20.7	22.6	7			25.1	24.7	12			22.7	22.2
18			16.5	- 18.8	3			9.9	9.1	8			51.0	- 42.2	13			14.3	- 12.7
20			8.3	8.1	4			9.9	- 9.4	9			9.0	9.4	14			20.2	- 20.3
0	2	3	168.7	162.3	7			9.9	9.5	12			9.0	9.2	15			16.0	- 17.8
1			94.3	96.5	8			19.0	- 15.5	15			23.3	20.2	0	2	5	9.6	15.1
3			5.0	- 5.3	9			9.9	- 8.9	1	3	4	7.2	- 9.4	1			13.6	13.0
4			35.6	31.0	10			13.2	- 11.4	2			7.2	7.8	2			43.3	- 44.4
5			32.3	- 30.3	11			13.2	11.9	3			11.6	9.2	4			56.9	62.3
6			19.0	- 19.2	16			9.9	10.4	5			9.0	- 7.8	5			8.8	- 10.8
7			59.5	- 60.5	1	7	3	19.0	- 18.4	6			17.9	14.9	6			16.0	- 18.4
8			20.7	18.7	3			14.9	- 14.6	7			13.4	13.8	7			12.8	12.4
9			26.5	- 27.4	4			19.0	18.9	9			13.4	14.2	8			20.0	- 22.0
10			21.5	- 22.5	5			9.9	- 14.4	11			13.4	- 10.7	9			46.5	46.3
11			16.5	- 16.6	6			26.5	- 30.0	13			13.4	12.4	11			60.1	56.6
12			38.9	- 38.7	7			21.5	- 23.6	15			23.3	- 17.6	12			33.6	28.8
13			54.6	- 57.5	8			13.2	14.0	0	4	4	37.5	- 35.9	13			41.7	38.0
14			9.1	- 8.3	9			13.2	11.2	1			15.2	13.7	14			4.8	5.4
15			43.0	- 44.6	10			35.6	- 34.0	3			14.3	- 5.6	1	3	5	31.6	- 32.2
18			11.6	13.4	11			19.0	- 16.7	4			13.4	- 11.6	2			39.9	39.9
19			43.0	41.3	13			38.0	32.2	5			57.3	49.3	3			61.5	- 68.8
20			48.0	- 51.0	14			38.9	- 35.5	9			41.2	39.8	5			24.1	- 23.0
1	3	3	177.0	161.0	0	8	3	81.9	96.3	12			11.6	8.8	6			54.0	- 49.2
2			67.8	- 60.7	1			49.6	54.3	13			23.3	17.3	7			11.6	13.1
3			6.6	- 9.8	3			19.0	18.4	15			41.2	33.2	8			39.1	- 37.8
4			25.6	24.5	4			19.0	14.9	1	5	4	51.0	- 48.7	9			21.6	19.9
5			43.0	- 46.3	5			14.9	- 14.1	2			44.8	- 48.7	10			102.2	102.5
6			89.3	89.6	6			8.3	- 10.4	3			51.0	- 53.4	12			54.0	- 48.9
7			45.5	48.8	7			52.9	- 57.6	5			31.3	- 31.9	13			20.8	- 21.4
9			20.7	- 22.3	8			32.3	29.5	6			27.7	30.5	14			7.5	6.3
10			49.6	56.4	11			25.6	- 24.0	7			31.3	36.5	0	0	6	36.6	38.4
11			13.2	- 10.4	12			20.7	- 23.6	9			13.4	- 15.9	1			89.7	- 89.5
12			25.6	- 31.0	1	9	3	62.9	72.2	10			75.1	- 72.3	4			22.4	- 23.8
13			86.8	- 87.7	2			20.7	- 25.3	11			62.7	53.3	5			28.3	27.0
14			89.3	93.4	3			9.9	- 9.2	13			51.0	- 43.1	6			11.6	11.1
15			56.2	50.5	6			30.6	36.9	14			11.6	13.0	7			62.3	59.2
16			24.0	- 17.5	7			14.9	17.7	15			44.8	42.4	9			18.3	19.4
18			30.6	- 28.3	9			8.3	- 12.3	0	6	4	9.0	- 8.1	1	1	6	58.8	- 57.5
19			48.0	- 46.5	0	10	3	20.7	- 30.6	1			68.9	- 60.5	3			22.7	- 19.8
0	4	3	111.6	-112.1	0	0	4	43.2	- 47.5	2			17.9	- 14.9	4			13.4	- 9.5
1			62.0	- 54.4	1			88.6	-114.8	3			29.5	31.7	7			29.4	- 29.9
3			44.7	42.4	2			13.4	- 20.0	4			83.2	72.0	9			26.9	28.3
4			43.0	- 42.8	3			49.2	57.2	5			17.9	- 16.9	0	2	6	12.0	11.2
5			24.0	22.6	4			96.7	105.3	6			13.4	13.2	1			12.0	- 7.3
6			8.3	11.2	5			17.9	- 15.3	7			13.4	- 11.8	2			12.0	11.1
7			30.6	30.1	6			13.4	17.9	8			60.9	- 55.0	3			33.6	- 33.3
9			35.6	38.4	7			37.6	- 35.1	9			62.7	- 53.4	4			11.2	- 10.2
10			20.7	22.8	8			70.7	- 69.7	11			65.3	- 57.7	6			18.4	- 19.0
11			14.9	16.8	9			55.5	- 51.2	12			39.4	38.7	7			21.6	- 20.3
12			25.6	24.0	11			93.1	- 95.9	13			33.1	- 37.5	8			8.8	7.7
13			25.6	29.0	12			70.7	70.5	14			7.2	- 5.7	4	3	6	18.3	16.4
14			9.9	9.7	13			37.6	- 38.6	1	7	4	39.4	32.7	7			5.8	- 8.4

of 1.0 for oxygen and 0.5 for silicon and magnesium were used as starting values.

Calculated structure factors were scaled to the observed values using different scale factors for different layers, and all observations were weighted as one. After several cycles of refinement during which atomic parameters, isotropic temperature factors and scale factors were allowed to vary, the R value, $(\Sigma||F_o|-|F_c||/\Sigma|F_o|)$, for the 680 observed reflections reached 0.095. An attempt to refine the structure further with anisotropic temperature factors was unsuccessful, showing that the experimental data were not sufficiently accurate to determine meaningful anisotropic temperature factors.

The final atomic parameters and temperature factors of orthoenstatite are given in Table 1. The comparison between F_o and F_c is given in Table 2. The interatomic distances and angles were computed on the IBM 7090 computer using program ORFFE (BUSING, MARTIN and LEVY, 1964) with the estimated standard deviations obtained in the structure refinement.

Table 3. *Interatomic distances and angles in orthoenstatite* $MgSiO_3$

within the Si(A) tetrahedron

Si(A)—O(1A)	1.614 (8) Å	O(1A)—O(2A)	2.752 (11) Å
—O(2A)	1.598 (8)	O(1A)—O(3A)	2.735 (12)
—O(3A)*	1.673 (10)	O(1A)—O(3A′)	2.636 (12)
—O(3A′)*	1.635 (10)	O(2A)—O(3A)	2.500 (12)
Mean	1.630	O(2A)—O(3A′)	2.682 (12)
		O(3A)—O(3A′)	2.626 (4)
		Mean	2.655

O(1A)—Si(A)—O(2A)		118.0 (5)°
O(1A)—	—O(3A)	112.6 (5)
O(1A)—	—O(3A′)	108.4 (5)
O(2A)—	—O(3A)	99.7 (5)
O(2A)—	—O(3A′)	112.1 (5)
O(3A)—	—O(3A′)	105.1 (3)
	Mean	109.3

within the Si(B) tetrahedron

Si(B)—O(1B)	1.619 (8) Å	O(1B)—O(2B)	2.746 (10) Å
—O(2B)	1.596 (9)	O(1B)—O(3B)	2.636 (12)
—O(3B)*	1.663 (10)	O(1B)—O(3B′)	2.664 (11)
—O(3B′)*	1.687 (9)	O(2B)—O(3B)	2.673 (12)
Mean	1.641	O(2B)—O(3B′)	2.590 (11)
		O(3B)—O(3B′)	2.758 (6)
		Mean	2.678

O(1B)—Si(B)—O(2B)		117.3 (5)°
O(1B)—	—O(3B)	106.9 (5)
O(1B)—	—O(3B′)	107.4 (5)
O(2B)—	—O(3B)	110.2 (5)
O(2B)—	—O(3B′)	104.2 (4)
O(3B)—	—O(3B′)	110.8 (3)
Mean		109.5

* Represent bridging oxygen atoms.

Table 3. *(Continued)*

within the M(1) octahedron

M(1)—O(1A)	2.136 (9) Å	O(1A)—O(1A′)	3.024 (9) Å
—O(1A′)	2.028 (9)	O(1A)—O(2A)	2.967 (12)
—O(1B)	2.150 (9)	O(1A′)—O(2A)	2.983 (13)
—O(1B′)	2.054 (9)	O(1A)—O(1B)	2.800 (11)
—O(2A)	2.002 (10)	O(1A′)—O(1B)	2.823 (11)
—O(2B)	2.051 (9)	O(1A)—O(1B′)	2.823 (11)
Mean	2.070	O(1A′)—O(2B)	2.757 (11)
		O(2A)—O(1B′)	2.804 (11)
		O(2A)—O(2B)	2.888 (12)
		O(1B)—O(1B′)	3.020 (9)
		O(1B)—O(2B)	3.122 (11)
		O(1B′)—O(2B)	3.076 (13)
		Mean	2.924

O(1A)—M(1)—O(1A′)		93.1 (3)°
O(1A)—	—O(2A)	91.6 (4)
O(1A′)—	—O(2A)	95.5 (4)
O(1A)—	—O(1B)	81.6 (3)
O(1A)—	—O(1B′)	84.7 (3)
O(1A′)—	—O(1B)	85.0 (4)
O(1A′)—	—O(2B)	85.1 (4)
O(2A)—	—O(1B′)	87.5 (4)
O(2A)—	—O(2B)	90.9 (4)
O(1B)—	—O(1B′)	91.8 (3)
O(1B)—	—O(2B)	96.0 (3)
O(1B′)—	—O(2B)	97.0 (4)
Mean		90.0

within the M(2) octahedron

M(2)—O(1A)	2.102 (9) Å	O(1A)—O(2A)	2.910 (13) Å
—O(1B)	2.081 (9)	O(1A)—O(3A)	3.577 (12)
—O(2A)	2.035 (10)	O(2A)—O(3A)	2.500 (12)
—O(2B)	1.984 (10)	O(1A)—O(1B)	2.800 (10)
—O(3A)	2.292 (9)	O(1A)—O(2B)	2.757 (11)
—O(3B)	2.453 (9)	O(2A)—O(1B)	2.804 (11)
Mean	2.158	O(2A)—O(3B)	3.037 (12)
		O(3A)—O(2B)	3.529 (12)
		O(3A)—O(3B)	2.884 (12)
		O(1B)—O(2B)	2.977 (13)
		O(1B)—O(3B)	3.201 (11)
		O(2B)—O(3B)	3.441 (13)
		Mean	3.035

Table 3. *(Continued)*

O(1A)—M(2)—O(2A)		89.4 (4)°
O(1A)—	—O(3A)	108.9 (4)
O(2A)—	—O(3A)	70.3 (4)
O(1A)—	—O(1B)	84.1 (3)
O(1A)—	—O(2B)	84.8 (4)
O(2A)—	—O(1B)	85.9 (4)
O(2A)—	—O(3B)	84.6 (3)
O(3A)—	—O(2B)	111.0 (4)
O(3A)—	—O(3B)	74.8 (3)
O(1B)—	—O(2B)	94.2 (3)
O(1B)—	—O(3B)	89.4 (3)
O(2B)—	—O(3B)	101.2 (3)
Mean		89.9

Si—Si distances		Si—O—Si angles	
Si(A)—Si(A)	3.047 (4) Å	Si(A)—O(3A)—Si(A)	134.2 (6)°
Si(B)—Si(B)	3.012 (4)	Si(B)—O(3B)—Si(B)	128.0 (5)

Discussion

The refined structure of orthoenstatite is not very different from that obtained by LINDEMANN (1961). Selected interatomic distances and angles are presented (Table 3).

1. Structure obtained

In orthoenstatite[1] two crystallographically distinct metal sites, M(1) and M(2), are occupied by Mg atoms. The octahedral coordination of oxygen atoms around M(1) is regular. The long bonds from M(2) to O(3A) (2.292 Å) and to O(3B) (2.453 Å) cause a large distortion in the M(2) octahedron. This distortion can be explained by the fact that O(3A) and O(3B) are each shared by two Si atoms. Each M(2) octahedron shares one edge [O(2A)—O(3A)] with a Si(A) tetrahedron.

Like clinoenstatite, orthoenstatite possesses two kinds of SiO_3 chains (Fig. 1). The Si(A) chains are more fully extended along c [O(3A′)—O(3A)—O(3A″) = 160.8°] than the Si(B) chains [O(3B′)—O(3B)—O(3B″) = 139.7°]. In all tetrahedra, the Si—O bonds are

[1] In this paper, the atom designation of BURNHAM (1967), is used for easy comparison between monoclinic and orthorhombic pyroxenes. The M(1) and M(2) sites are the same as in hypersthene (GHOSE, 1965) and correspond respectively to the MII and MI sites in clinoenstatite (MORIMOTO *et al.*, 1960).

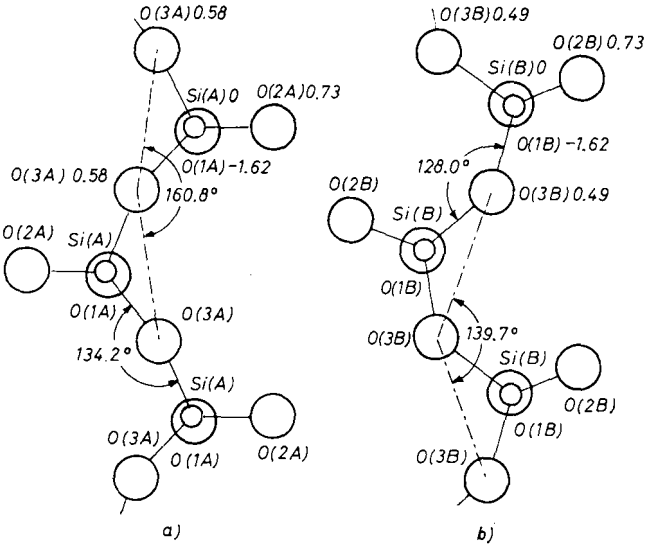

Fig. 1. Two different silicate chains in the structure of orthoenstatite projected on (100). Numbers represent distances in Å above and below (negative) a plane passed through the Si atoms. Compare the silicate chains in pigeonite (Fig. 6 of MORIMOTO *et al.*, 1960)

significantly longer to chain-linking oxygen atoms [O(3A) and O(3B)] than to other oxygen atoms.

In general, the Mg coordination and the SiO_3 chains in orthoenstatite retain the characteristics of clinoenstatite and orthopyroxenes previously described.

2. Structural relations of orthoenstatite and clinoenstatite

The structure of clinoenstatite was determined from two-dimensional data (MORIMOTO *et al.*, 1960). Although the atomic parameters of clinoenstatite are not as accurate as those of orthoenstatite, it is possible to obtain some conclusions about the geometric relationship between the structures of the two polymorphs.

The structures of orthoenstatite and clinoenstatite, as can be seen from their projections on to (010) (Fig. 2), are composed of identical structural units: two kinds of layers, made up of silicate chains and Mg octahedra parallel to (100). The difference between the two structures arises from the stacking of the structural units (MORIMOTO, 1959). A part of each structure with a layer of the Si(A) chains[2] and

[2] In the structure of clinoenstatite (MORIMOTO *et al.*, 1960), the Si(A) and Si(B) chains are called SiI and SiII chains respectively.

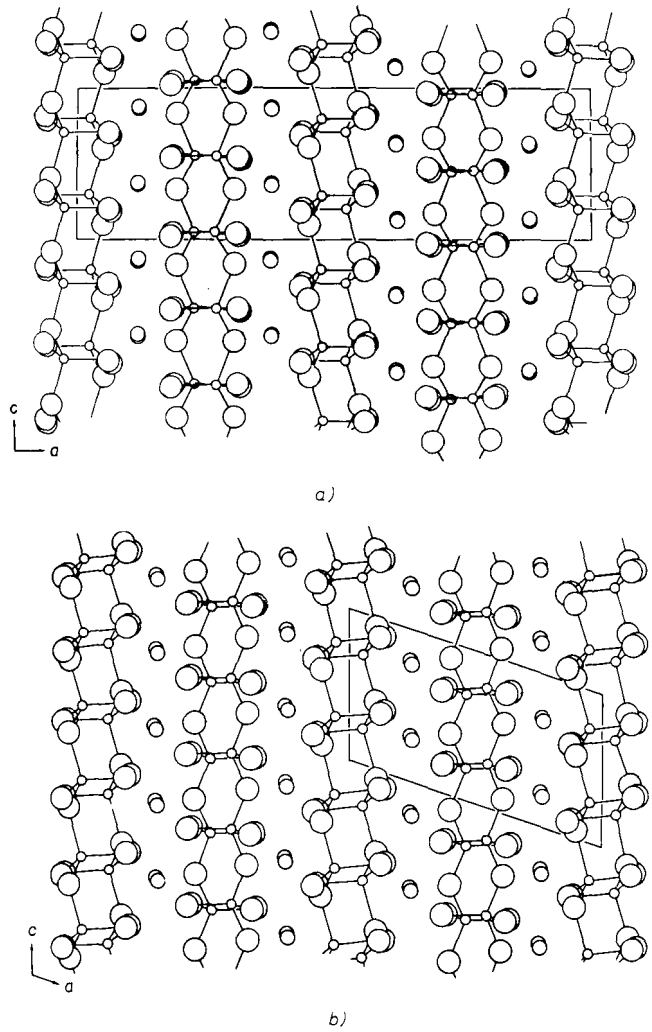

Fig. 2. Comparison of the structures of orthoenstatite (*a*) and clinoenstatite (*b*) projected on (010). A unit cell is outlined in each figure

a band of Mg octahedra is projected on (100) for orthoenstatite and clinoenstatite along the a^* axis (Fig. 3). The difference of the two structures is clearly illustrated in the arrangement of the Si(A) chains in the same layer. The Si(A) chains are related by a *b*-glide plane (100) in orthoenstatite, but not in clinoenstatite.

In order to examine the validity of the cell twinning proposed by Ito (1935, 1950), a *hypothetical* orthoenstatite structure is constructed

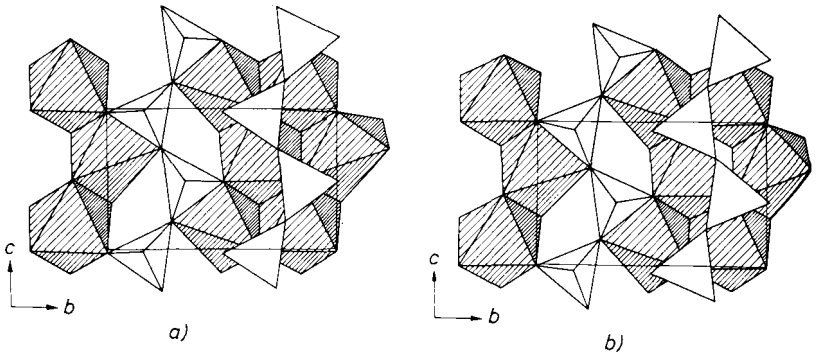

Fig. 3. Part of the crystal structure with the layer of Si(A) chains and the band of Mg octahedra of orthoenstatite (*a*) and clinoenstatite (*b*) projected on (100) along the a^*. Notice the difference in the relationship between the Si(A) chains in each structure. The Si(A) chains are related by a *b*-glide plane (100) through the Si chains in orthoenstatite, but not in clinoenstatite

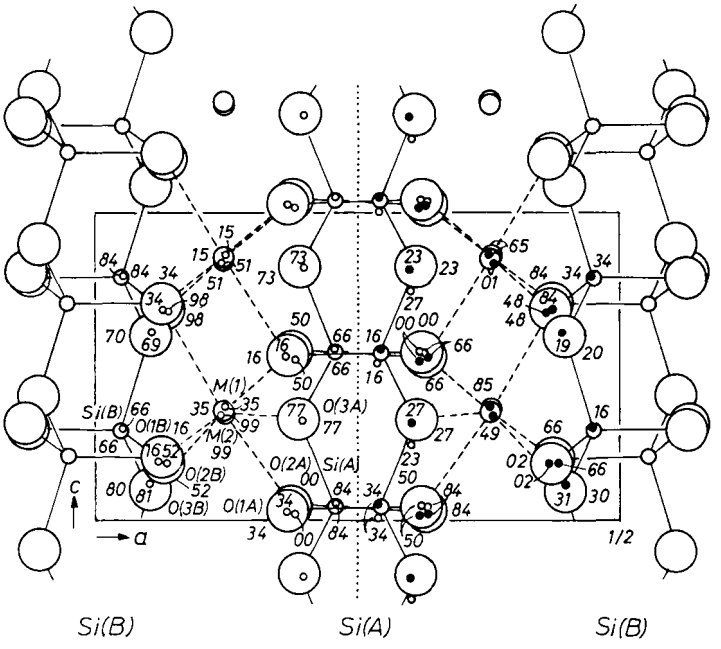

Fig. 4. Orthoenstatite structure (large circles) is compared with a hypothetical structure (small circels, open in the left and solid in the right of the glide plane) constructed by glide-reflecting the clinoenstatite structure (small open circles), assuming a glide plane (100) with $b/2$ translation passed through the Si(A) chains. All structures are projected on (010) along the direction of b. Only one half of the unit cell of orthoenstatite is given

y glide reflecting the clinoenstatite structure in a *b*-glide plane 100) passed through the Si(A) chains, and is compared with the real thoenstatite structure, in (010) projection (Fig. 4). The *hypothetical* ll dimensions of $a = 18.24$, $b = 8.81$, and $c = 5.17$ Å, are in complete greement with the observed values: $a = 18.22$, $b = 8.81$, and = 5.17 Å. The differences of the fractional atomic coordinates etween *hypothetical* and real orthoenstatites (Table 4) are within the mits of accuracy of the clinoenstatite structure except for the $\Delta(Z/c)$ ifferences of M(2) and O(2A), which however only amount to about .12 Å. The agreement between the structures is shown on Fig. 4, where he observed sites appear as large circles and the theoretical ones as small ircles (open on the left and solid on the right of the glide plane).

In fact, the arrangements of the nearest oxygen atoms around i and Mg are identical in the two polymorphs, but the arrangements

Table 4. *Fractional atomic coordinates in hypothetical orthoenstatite (upper) and in real orthoenstatite (lower)*

	x/a	$\Delta(x/a)$	y/b	$\Delta(y/b)$	z/c	$\Delta(z/c)$
M(1)	0.376		0.653		0.864	
	0.376	0.000	0.654	−0.001	0.866	−0.002
M(2)	0.379		0.486		0.335	
	0.377	0.002	0.485	0.001	0.361	−0.026
i(A)	0.271		0.342		0.060	
	0.272	−0.001	0.341	0.001	0.049	0.011
i(B)	0.473		0.339		0.795	
	0.474	−0.001	0.337	0.002	0.799	−0.004
O(1A)	0.181		0.344		0.031	
	0.183	−0.002	0.339	0.005	0.035	−0.004
O(2A)	0.311		0.502		0.018	
	0.312	−0.001	0.502	0.000	0.043	−0.025
O(3A)	0.302		0.225		−0.169	
	0.304	−0.002	0.225	0.000	−0.170	0.001
O(1B)	0.562		0.341		0.816	
	0.563	−0.001	0.338	0.003	0.801	0.015
O(2B)	0.431		0.482		0.683	
	0.434	−0.003	0.484	−0.002	0.688	−0.005
O(3B)	0.447		0.187		0.612	
	0.447	0.000	0.196	−0.009	0.600	0.012

of the second neighbors are different. The Si—O distances in clinoen statite, with mean values of 1.64 Å for the Si(A) and 1.66 Å for th Si(B) tetrahedra (MORIMOTO *et al.*, 1960), seem to be slightly large than those in orthoenstatite where the mean values are 1.630 Å fo the Si(A) and 1.641 Å for the Si(B) tetrahedra. The standard deviatio of the mean Si—O distances, however, is 0.03 Å in the clinoenstatit structure so that the differences in Si—O distances between tw polymorphs can not be considered significant. The average M(1)—O and M(2)—O distances are the same in both structures, equal t

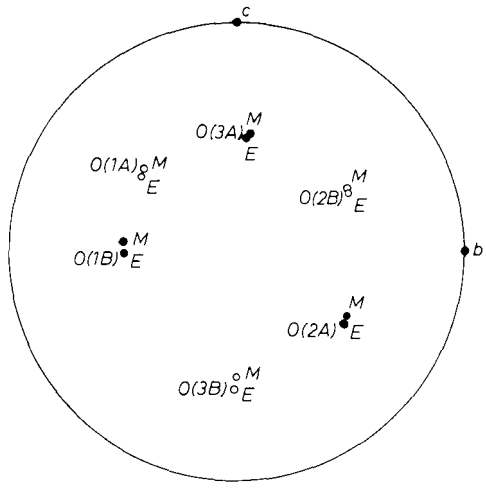

Fig. 5. Coordination around the M(2) site in orthoenstatite and clinoenstatit represented in the stereogram. M(2) site is at center of sphere of projection M and E represent the coordination in clinoenstatite and in orthoenstatit respectively

2.07 and 2.15 Å respectively. Because of the $\angle(Z/c)$ of the M(2) site the bond angles of the M(2) octahedron differs slightly from on polymorph to the other, as shown in stereographic projection (Fig. 5).

Thus orthoenstatite is considered as cell twinning of clinoenstatit in the strict sense of the word as introduced by ITO (1935, 1950). These polymorphic relationships of $MgSiO_3$ represent an importan characteristic in transition of some silicate minerals from the structur viewpoint. In these minerals, the structure and dimensions of th structural units do not change by transition, and the polymorphis can be expressed by different symmetry operations on the structur units.

It is obvious from the above discussions that the difference in the stacking of the structural units in the two polymorphs is quite similar to the difference of stacking in polytypes. It is, therefore, very likely that the structural units in orthoenstatite might also occupy the positions which they occupy in clinoenstatite by mistake. The observations of diffuse reflections along the a^* axis, reported on meteoritic and heated terrestrial orthoenstatites (BROWN and SMITH, 1963; POLLACK and RUBLE, 1964), indicate the existence of stacking mistakes in some orthoenstatites. However, no diffuse reflections are observed with the Bishopville orthoenstatite and this indicates the ordered arrangement of the structural units without stacking mistakes.

It is of interest to examine whether the structure of diopside can be cell-twinned on (100) as in clinoenstatite resulting in an orthorhombic structure. As easily observed from the diopside structure, the application of the b-glide plane creates large distortions of silicon tetrahedra in the chains. In other words, distortion of silicon tetrahedra is indispensable in the orthorhombic structure as long as the eight coordination of Ca is maintained. In order to keep the silicon tetrahedra reasonably regular in the orthorhombic structure, the coordination of Ca must be changed as in orthoenstatite. This simple geometric relation may explain why diopside has no orthorhombic polymorph and why orthopyroxenes cannot accommodate as much calcium as clinopyroxenes.

3. Structural relations of orthoenstatite to hypersthene and orthoferrosilite

On comparing the structures of orthoenstatite, hypersthene (GHOSE, 1965) and orthoferrosilite (BURNHAM, 1967), the general features of the structures are in agreement.

The mean interatomic distances, M—O, of both M(1) and M(2) octahedra increase with the amount of Fe replacing Mg. The changes of the mean interatomic distances of r [M(1)—O] and r [M(2)—O] are shown (Fig. 6). The estimated standard deviations of the mean M—O distances for orthoenstatite and orthoferrosilite, caluculated by dividing the average standard deviations of the M—O distances by the square root of the number of independent bonds in the octahedra around M(1) and M(2), are 0.005 Å for M(1)—O and 0.004 Å for M(2)—O. Thus the difference of the mean M—O distances in the three orthopyroxenes is significant. Based on the values of orthoenstatite

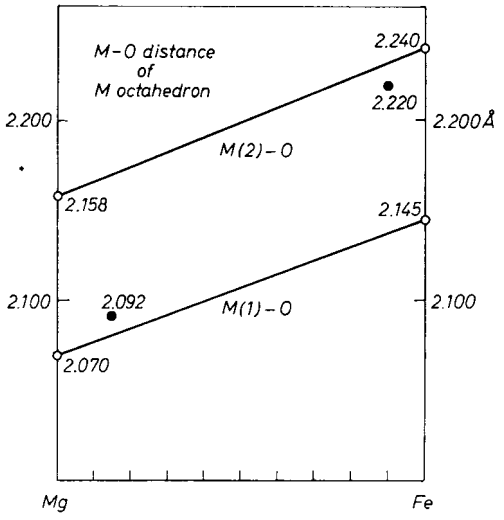

Fig. 6. Change of the mean M—O distances (in Å) in the orthopyroxenes due to Mg:Fe ratio at the M sites. The mean M—O distances in hypersthene (GHOSE, 1965) are denoted by solid circles and given at the composition representing the metal distribution at the M(1) and M(2) sites

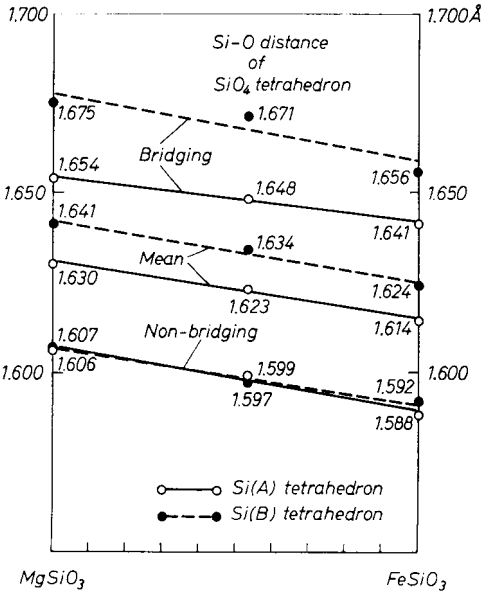

Fig. 7. Change of the mean Si—O distances (in Å) in the orthopyroxenes along $MgSiO_3$—$FeSiO_3$ system. Full line: Si(A) tetrahedra, dotted line: Si(B) tetrahedra

and orthoferrosilite, the mean M—O distances are given by the following equations:

$$r\,[\mathrm{M(1)—O}] = 2.070 + 0.075\,X,$$

and

$$r\,[\mathrm{M(2)—O}] = 2.158 + 0.082\,X,$$

where X is the mole percent ferrosilite.

The above relations may be used to determine the Mg:Fe ratio in the M(1) and M(2) sites in orthopyroxenes. GHOSE (1965) reported that the Mg:Fe ratio in the hypersthene is 85:15 for the M(1) sites and 10:90 for the M(2) site. The mean interatomic distances of M(1)—O and M(2)—O in his structure interpolated with the curves in Fig. 6, however, indicate different Mg:Fe ratios with 73:27 for the M(1) site and 24:76 for the M(2) site yielding a total composition of $En_{48}Fs_{52}$, which is the composition of the hypersthene. These results are in good agreement with those obtained in the study by the Mössbauer effect (BANCROFT, BURNS and HOWIE, 1967) for a charnockitic hypersthene with 48.4 percent iron, which indicate that about 25 percent and 72 percent of the M(1) and M(2) positions, respectively, are occupied by iron.

As for the SiO_3 chains in the orthopyroxenes, there are two crystallographically distinct kinds, consisting of Si(A) and Si(B) tetrahedra. In both tetrahedra, the bridging bonds are significantly different from the non-bridging bonds in length (Table 3). It is of interest to notice that the mean lengths of the bridging bond is different in the two tetrahedra, but the mean lengths of the non-bridging bonds is the same for both tetrahedra, indicating that the minimum value for the Si—O distances is constant in each structure of orthopyroxenes.

Another aspect of interest is the change of the Si—O distances due to replacement of Mg by Fe in orthopyroxenes. The increase of Fe substitution decreases the Si—O distances linearly (Fig. 7). Since the estimated standard deviations of the mean Si—O distances, calculated in the same way as those of the mean M—O distances, are 0.005 Å in orthoenstatite and orthoferrosilite, the differences of the mean Si—O distances for both structures, 0.016 Å for the Si(A) tetrahedron and 0.017 Å for the Si(B) tetrahedron, are considered fairly significant. This is also supported by the fact that the corresponding Si—O distances change linearly with almost the identical inclination in the three structures of orthopyroxenes, each of which was refined by different investigations.

The bond angles O—Si—O are in good agreement in the structures of orthopyroxenes. The bond angle O(1)—Si—O(2) has a large value of about 117° for the three structures as in other metasilicates with silicate chains (MCDONALD and CRUICKSHANK, 1967).

The effects of substitution between Mg and Fe on the interatomic distances could be explained on the basis of a larger ionic radius and a greater electronegativity of Fe than of Mg. These data for orthopyroxenes are probably the first examples that the size of the SiO_4 tetrahedron is influenced not only by the linkage type of the SiO_4 tetrahedron but also by the kinds of large metal ions outside the tetrahedron (SMITH and BAILEY, 1963).

The change of the Si—O distances by the substitution between Mg and Fe has not been observed as far as we notice in the amphiboles and micas. This is considered to be due to the fact that the substitution between Si and Al in the SiO_4 tetrahedra, and the packing geometry of oxygen atoms have more distinct influences on the Si—O distances than the substitution between Mg and Fe in the amphiboles and micas.

Acknowledgements

We are indebted to Professor T. ITO for his interest and encouragements. We are also indebted to Professor J. D. H. DONNAY, Dr. G. DONNAY and Dr. L. FINGER for reviewing the manuscript and providing numerous suggestions for its improvement.

Computations were performed in part on the IBM 7090 computer through the UNICON project and in part on HITAC 5020 at the University of Tokyo. Part of the expenses of this study was defrayed by a grant for scientific research from the Ministry of Education of the Japanese Government.

Added in proof: Careful Mössbauer work by VIRGO and HAFNER (S. S. HAFNER, private communication, 1968) on the orthopyroxene used by GHOSE (1965) confirmed the site occupancy factors obtained by the previous x-ray work. In view of this fact, a non-linear relationship is probable in the (Mg, Fe)–O distances.

References

G. M. BANCROFT, R. G. BURNS and R. A. HOWIE (1967), Determination of the cation distribution in the orthopyroxene series by the Mössbauer effect. Nature **213**, 1221—1223.

M. G. BOWN and P. GAY (1957), Observations on pigeonite. Acta Crystallogr. **10**, 440—441.

F. R. BOYD and J. F. SCHAIRER (1964), The system $MgSiO_3$—$CaMgSi_2O_6$. Jour. Petrology **5**, 275—309.

W. L. Brown, N. Morimoto and J. V. Smith (1961), A structural explanation of the polymorphism and transitions of $MgSiO_3$. Jour. Geol. **69**, 607—616.

W. L. Brown and J. V. Smith (1963), High-temperature x-ray studies on the polymorphism of $MgSiO_3$. Z. Kristallogr. **118**, 186—212.

Charles W. Burnham (1967), Ferrosilite. Carnegie Inst. Wash. Year Book **65**, 285—290.

W. R. Busing, K. O. Martin and H. A. Levy (1962), ORFLS, a FORTRAN crystallographic least squares program. U. S. Atomic Energy Commission Report No. ORNL-TM-305.

W. R. Busing, K. O. Martin and H. A. Levy (1964), ORFFE, a FORTRAN crystallographic function and error program. Oak Ridge National Laboratory, Oak Ridge, Tennessee.

A. Byström (1943), Röntgenuntersuchung des Systems $MgO—Al_2O_3—SiO_2$. Ber. dtsch. Keram. Ges. **24**, 2—15.

S. Ghose (1965), $Mg^{2+}—Fe^{2+}$ order in an orthopyroxene, $Mg_{0.93}Fe_{1.07}Si_2O_6$. Z. Kristallogr. **122**, 81—99.

International tables for x-ray crystallography (1962), **3**, 202. Kynoch Press, Burmingham.

T. Ito (1935), On the symmetry of the rhombic pyroxene. Z. Kristallogr. **90**, 151—162.

— (1950), X-ray studies of polymorphism, pp. 30—41. Maruzen, Tokyo.

W. Lindemann (1961), Beitrag zur Enstatitstruktur (Verfeinerung der Parameterwerte). N. Jahrb. Min., Mh., 226—233.

W. S. McDonald and D. W. J. Cruickshank (1967), A refinement of the structure of sodium metasilicate. Acta Crystallogr. **22**, 37—43.

N. Morimoto (1956), The existence of monoclinic pyroxenes with the space group $C_{2h}^5—P2_1/c$. Proc. Jap. Acad. **32**, 750—752.

— (1959), The structural relations among three polymorphs of $MgSiO_3$—enstatite, protoenstatite, and clinoenstatite. Carnegie Inst. Wash. Year Book **58**, 197—198.

N. Morimoto, D. E. Appleman and H. T. Evans (1960), The crystal structures of clinoenstatite and pigeonite. Z. Kristallogr. **114**, 120—147.

S. S. Pollack and W. D. Ruble (1964), X-ray identification of ordered and disordered ortho-enstatite. Amer. Miner. **49**, 983—992.

C. B. Sclar, L. C. Carrison and C. M. Schwartz (1964), High-pressure stability field of clinoenstatite and the orthoenstatite-clinoenstatite transition. Trans. Amer. Geophys. Union, **45**, program of 46th Annual Meeting, 121.

J. V. Smith and S. W. Bailey (1963), Second review of Al—O and Si—O tetrahedral distances. Acta Crystallogr. **16**, 801—811.

D. A. Stephenson, C. B. Sclar and J. V. Smith (1966), Unit cell volumes of synthetic orthoenstatite and low clinoenstatite. Min. Mag. **40**, 838—846.

H. E. Swanson, N. T. Gilfrich and M. I. Cook (1956), Standard x-ray diffraction powder patterns. Nat. Bur. Stand. Circular 539, **6**, 32.

S. E. Warren and W. L. Bragg (1928), The structure of diopside, $CaMg(SiO_3)_2$. Z. Kristallogr. **69**, 168—193.

S. E. Warren and D. I. Modell (1930), The structure of enstatite, $MgSiO_3$. Z. Kristallogr. **75**, 1—14.